

Removal of fluoride from aqueous phase by biosorption onto algal biosorbent *Spirogyra* sp.-IO2: Sorption mechanism elucidation

S. Venkata Mohan*, S.V. Ramanaiah, B. Rajkumar¹, P.N. Sarma

Bioengineering and Environmental Centre, Indian Institute of Chemical Technology, Hyderabad 500007, India

Received 3 May 2006; received in revised form 4 July 2006; accepted 5 July 2006

Available online 10 July 2006

Abstract

This communication presents results pertaining to the adsorptive studies carried out on fluoride removal onto algal biosorbent (*Spirogyra* IO2). Batch sorption studies were performed and the results revealed that biosorbent demonstrated ability to adsorb the fluoride. Influence of varying the conditions for removal of fluoride, such as the fluoride concentration, the pH of aqueous solution, the dosage of adsorbent, the temperature on removal of fluoride, and the adsorption–desorption studies were investigated. Sorption interaction of fluoride on to algal species obeyed the pseudo first order rate equation. Experimental data showed good fit with the Langmuir's adsorption isotherm model. Fluoride sorption was found to be dependent on the aqueous phase pH and the uptake was observed to be greater at lower pH. Maximum fluoride sorption was observed at operating 30 °C operating temperature. Adsorption–desorption of fluoride into inorganic solutions and distilled water was observed and this indicated the combined effect of ion exchange and physical sorption phenomena. Significant changes in the FT-IR spectra was observed after fluoride sorption which is indicative of the participation of surface function groups associated with hydrogen atoms in the carboxylic groups in sorption interaction. From X-ray photoelectron spectroscopy (XPS) analysis a marginal increase in the area for the binding energy peak at 287.4 eV was observed which could be due to the formation of –C–F– bonds. Thermogravimetric (TGA) analysis of the fluoride loaded sorbent showed that the biosorbent underwent three steps decomposition process when heated from 25 to 100 °C. The maximum weight loss was observed to be between 200 and 400 °C and 700 and 800 °C.

© 2006 Elsevier B.V. All rights reserved.

Keywords: Biosorption; Algae; *Spirogyra*; Biosorbent; Kinetics; Adsorption–desorption; Isotherms; SEM; FT-IR; XPS; TGA

1. Introduction

Fluoride ion in water exhibits unique properties, as its concentration in optimum dose in drinking water is advantageous to health and excess concentration beyond the prescribed limits affects the health [1]. High fluoride concentration in the ground water and surface water in many parts of the world is a cause of great concern. High fluoride in drinking water was reported from different geographical regions. The problem of excessive fluoride in ground water in India was first detected in Nellore (part of Prakasam district now) of Andhra Pradesh in 1937 [2]. According to an estimate, 25 million people in 19 states and union territories have already been effected and another 66 mil-

lion are at risk including 6 million children below the age of 14 years [3]. Though fluoride enters the body mainly through water, food, industrial exposure, drugs cosmetics, etc. drinking water is the major source (75%) of daily in take [4]. A fluoride ion is attracted by positively charged calcium in teeth and bones, due to its strong electro negativity. Major health problems caused by fluoride are dental fluorosis (teeth mottling) skeletal fluorosis (deformation of bones in children and also in adults) and non skeletal fluorosis [5,6]. It can interfere with carbohydrates, lipids, protein, vitamins, enzymes and mineral metabolism when the dosage is high. In some parts of India, the fluoride levels are below 0.5 mg/l, while at certain other places, fluoride levels are as high as 35 mg/l [7,8].

De-fluoridation was reported by adsorption [9], chemical treatment [10,11], ion exchange [12], membrane separation [13,14], electrolytic de-fluoridation [15], and electro dialysis [16–18], etc. Among various processes, adsorption was reported to be effective [19]. Investigators reported various types of adsorbents namely activated carbon, minerals, fish bone char-

* Corresponding author. Tel.: +91 40 2716 3159.

E-mail addresses: vmohan_s@yahoo.com (S. Venkata Mohan), sarma1950@yahoo.com (P.N. Sarma).

¹ Department of Botany, Osmania University, Hyderabad 500007, India.

coal, coconut shell carbon and rice husk carbon, with different degrees of success [9,20–24]. Recently considerable interest was observed on the application of biosorbent materials for removal of various pollutants. Biosorbent materials can passively bind large amounts of metal(s) or organic pollutants, a phenomenon commonly referred to as biosorption [25–32]. Biosorbents are attractive since naturally occurring biomass(es) or spent biomass(es) can be effectively utilized [25]. Besides this, biosorption offers advantages of low operating cost, minimization of the volume of chemical and/or biological sludge to be disposed, high efficiency in dilute effluents, no nutrient requirements and environmental friendly and economical viable. It provides a cost-effective solution for industrial wastewater management [33]. Application of biosorbents/biomass from various microbial sources, leaf based adsorbents and water hyacinth was reported by various investigators [34–42]. Limited number of studies were available on the treatment by algal species (fresh and marine water) in spite of their ubiquitous distribution and their central role in the fixation and turnover of carbon [43–45]. Keeping the above points in view, batch adsorption of studies was carried out on the sorption of fluoride from aqueous phases using commonly available algal *Spirogyra*. The adsorption studies carried out under various experimental conditions and the results obtained are presented in this communication. The sorption mechanism elucidation was also carried out by employing instrumental techniques, viz., X-ray photoelectron spectroscopy (XPS), Fourier transform infra red spectroscopy (FT-IR), thermo gravimetric analysis (TGA) and scanning electron microscope (SEM). Algae are traditionally a food supplement and are generally safe. The algal *Spirogyra* species used as biosorbent in this experiment is generally grows profusely in nature ponds and its availability is easy without any practical investment. Thus using *Spirogyra IO2* as biosorbent is environmentally safe and practically economical.

2. Experimental

2.1. Chemicals

Stock solution of fluoride was prepared by dissolving 2.21 g of sodium fluoride (AR grade) in 1000 ml of double glass distilled water. The stock solution was then appropriately diluted to get the test solution of desired fluoride concentration.

2.2. Biosorbent

A viable form of algal species related to *Spirogyra IO2* species was studied as biosorbent to evaluate its potential to adsorb fluoride from aqueous phase. The algal biomass was collected from ponds in the premises of Osmania University campus, Hyderabad, India. The collected biomass was dewatered, cleaned and washed with de-ionized water initially and subjected to drying under diffused sunlight for a period of 7 days. Dried algal biomass was crushed to particle size of 1–2 mm. As the biosorption process involved mainly cell surface sequestration, cell wall modification could greatly alter the adsorption capability. A number of methods were employed for

cell wall modification of microbial cells in order to enhance the metal binding capacity of biomass and to elucidate the mechanism of biosorption [26,47]. Acid pretreatments were suggested in the literature to modify the surface characteristics/groups either by removing or masking the groups or by exposing more adsorption-binding sites [46–48]. The biomass particles were further treated with (0.1N HCl) for 8 h and subsequently, washed with distilled water twice before drying (24 h).

2.3. Batch sorption experiments

Batch sorption experiments were performed adopting bottle-point method as described by Venkata Mohan et al. [19]. In this method, each independent bottle represented one point on the graph containing the adsorbent and fluoride mixture in order to get accurate results. A series of 250 ml Stoppard glass bottles with 0.1 g of biosorbent were taken and 100 ml of solution containing fluoride concentration of 5, 10, 15, 20 and 25 mg F⁻/l were added in separate bottles and the adsorption mixture was agitated for a pre-determined time period (480 min) using horizontal shaker [temperature, 30 °C; agitation, 100 rpm; biosorbent mass, 0.1 g⁻¹; contact (equilibrium contact time), 120 min; desorption time, 60 min; pH 7.0]. Sorption kinetics were determined by analyzing uptake of the fluoride from aqueous solution at different time intervals of 15, 30, 60, 120, 180, 240, 300, 360, 420 and 480 min. Influence of temperature on the fluoride sorption was evaluated by placing five separate bottles in temperature control orbital shaker at 10, 20, 30, 40 and 50 °C [agitation, 100 rpm; biosorbent mass, 0.1 g⁻¹; concentration, 5 mg F⁻/l; contact (equilibrium contact time) time, 120 min; pH 7.0], respectively. Isothermal studies to determine the sorption capacity and intensity were carried out by adding various doses of sorbent (0.1–0.5 g at an increment of 0.1 g) and agitating the reaction mixture for the equilibrium time [temperature, 30 °C; agitation, 100 rpm; biosorbent mass, 0.1 g; concentration, 5 mg F⁻/l; adsorption (contact) time, 120 min; desorption time, 60 min; pH 7.0]. Influence of the aqueous phase pH on fluoride sorption was studied by adjusting the reaction mixture to different initial pH values from 2 to 10.5 (concentration, 5 mg F⁻/l; biomass, 0.1 g; temperature, 30 °C; agitation, 100 rpm; contact time, 120 min). Three separate adsorption–desorption experiments were carried for each of the desorption solvent used (distilled water, 0.1N HCl and 0.1N NaOH) separately up to three cycle. A single cycle sequence consist of adsorption (120 min) followed by desorption (60 min) [temperature, 30 °C; agitation, 100 rpm; biosorbent mass, 0.1 g; concentration, 5 mg F⁻/l; adsorption (contact) time, 120 min; desorption time, 60 min]. After adsorption, the resultant fluoride loaded algal biomass was filtered and air dried for a period of 5 min and reintroduced into the required desorption solvent and agitated.

2.4. Analysis

The residual fluoride concentration in the aqueous phase was analyzed colorimetrically using SPADNS method on a UV–vis

spectrophotometer (CE2021 2000 Series) according to the procedures outlined in Standard methods of APHA [49]. FT-IR spectra of *Spirogyra* were obtained by using a Thermo Nicolet Nexus 670 FT-IRS Spectrometer by KBr (0.1 g) keeping of dry biomass (0.1 g). Elemental analysis was done on Elemental Analyzer (Vario EL instrument). Particle size analysis was done on (Malvern) Master sizer 2000. TGA measurements were carried out on a Mettler Toledo (TGA/SDTA 851^c) instrument. X-ray photoelectron spectroscopy (XPS) was performed on a Kratos Analytical (AXIS 165). For scanning electron microscope, biosorbent sample was washed with 0.9% NaCl solution followed by phosphate buffer (pH 7.0) and subsequently the biomass was incubated in 3% glutaraldehyde (2 h). Incubated culture was serially treated with 10–90% alcohol for dehydration after transferred into absolute alcohol and subjected to SEM (Hitach S-3000N) analysis.

3. Results and discussion

3.1. Characterization of the biosorbent

3.1.1. Surface area and composition

Specific surface area of acid treated biosorbent (*Spirogyra IO2*) was observed to be $0.154 \text{ m}^2/\text{g}$ as determined by particle size analysis. The particle size distribution of the biosorbent ($10\% < 20 \mu\text{m}$, $50\% < 95 \mu\text{m}$, $90\% < 460 \mu\text{m}$) is depicted in Fig. 1. The algal biosorbent subjected to elemental analysis showed composition of N 2.36%, C 28.81%, S 1.33%, and H 3.14%.

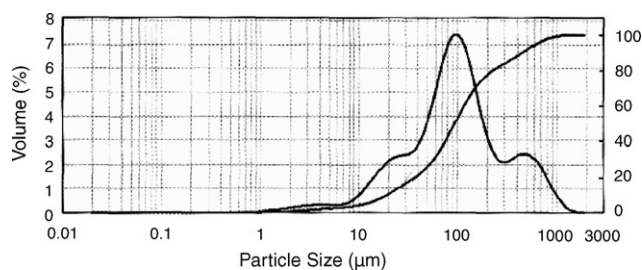


Fig. 1. Particle size analysis of biosorbent before sorption.

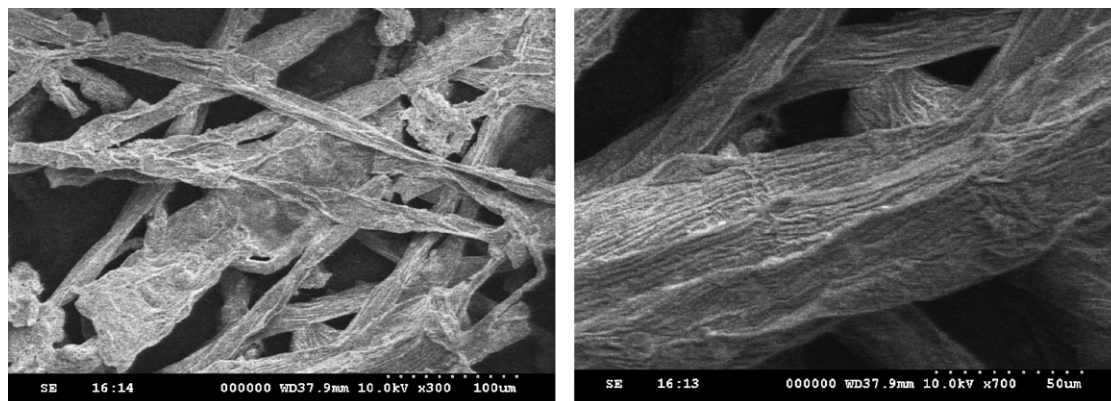
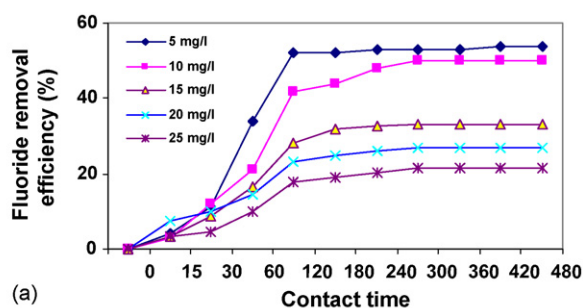
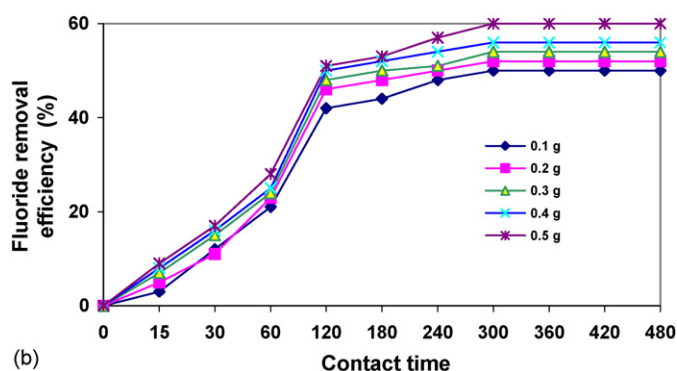


Fig. 2. Morphological (SEM image) details of biosorbent *Spirogyra* sp.-*IO2* before fluoride sorption.



(a)



(b)

Fig. 3. Variation of fluoride sorption by *Spirogyra* sp.-*IO2*. (a) Influence of contact time on the sorption capacity [temperature, 30°C ; agitation, 100 rpm; biosorbent mass, 0.1 g; pH 7.0]. (b) Influence of dose on the sorption capacity [temperature, 30°C ; agitation, 100 rpm; concentration, $5 \text{ mg F}^-/\text{l}$; pH 7.0; contact time, 120 min].

3.1.2. Surface morphology

The scanning electron micrograph clearly revealed the surface texture and morphology of the biosorbent (Fig. 2). It was evident from the micrographs that the biosorbent showed a well-defined rod clusters in net/mat format ($300\times$). At $700\times$ magnification, the single rod of the biosorbent was focused, where an uneven surface texture along with lot of irregular surface format was observed.

3.2. Sorption kinetics

The effect of contact time and sorptive removal of fluoride was depicted in Fig. 3(a). The rate of fluoride removal

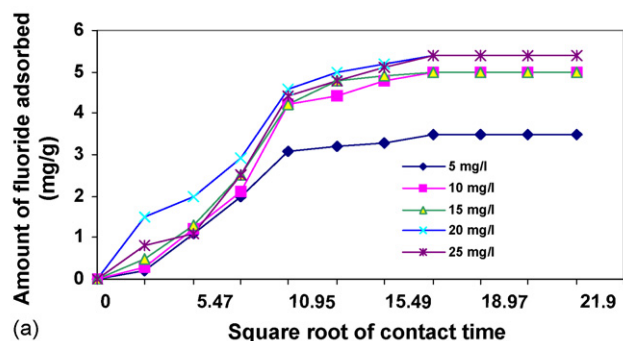
was rapid initially and then slowed down gradually until it attained equilibrium. Beyond which there was no significant increase in the rate of removal. The initial rapid sorption was perhaps due to participation of specific functional groups and active surface sites [50] in the adsorptive removal of the fluoride ion. A large fraction of the fluoride ion was removed within 120 min of the contact time in all the experimental variations studied, the fluoride removal efficiency showed a decreasing trend (gradually from 62 to 17.5% with increase in the aqueous phase fluoride concentration from 5 to 25 mg/l). The amount of fluoride adsorbed per unit mass of algae showed increasing trend up to 20 mg/l of fluoride concentration and subsequently decreased. It can be presumed from the data that the system showed higher removal rates up to 20 mg/l of fluoride concentration in aqueous phase. The effect of the dosage of algal *Spirogyra* on the sorption of fluoride was studied at 5 mg/l of fluoride concentration Fig. 3(b). Fluoride ion sorption increased concentration with the increasing dosage of sorbent. The highest percentage removal was observed at 0.5 g of biomass. The sorption kinetic data obtained from fluoride algal system was studied with different kinetic models [51,52] namely the intraparticle diffusion model [19,50,52] the pseudo first order [52] and the pseudo second order [52] models. The sorption kinetic data were correlated with the linear forms of the three models, respectively.

3.2.1. Intraparticle diffusion model

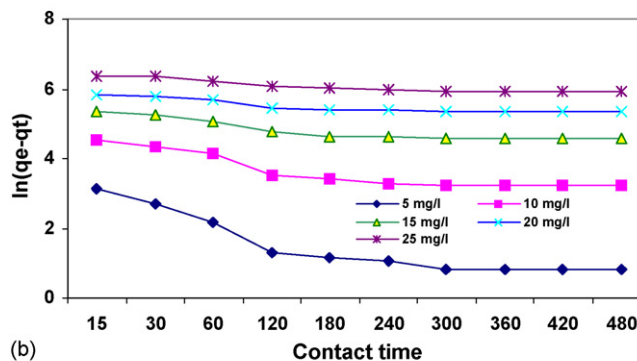
The basic assumption with intraparticle diffusion model is that the film diffusion was negligible and intraparticle diffusion was the only rate-controlling step [19,50,52]. The mathematical expression for the intraparticle diffusion model [41] might be represented as

$$q_t \approx k_p t^{0.5} \quad (1)$$

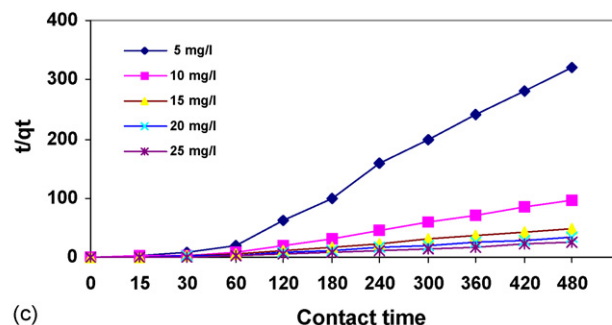
where q_t represents intraparticle diffusion rate constant and represents the fraction of fluoride removed (mg/g), k_p (mg/g min^{-0.5}) and t to denotes contact time (min). According to Eq. (1) the plot of fraction of fluoride removal (q_t) versus the square root of contact time ($t^{0.5}$) would yield a straight line passing through the origin if the adsorption process obeyed the intraparticle diffusion model. Sorption kinetic data was processed to determine whether intraparticle diffusion was rate limiting (Fig. 4(a)). The plots obtained were of general type, i.e., initial curved portion with a final linear portion. The initial curved portions might be attributed to the boundary layer diffusion effect [53], while the final linear portions might be due to intraparticle diffusion effects [53,54]. It might be observed, from the figure, that the straight line did not pass through the origin and this further indicated that the intraparticle diffusion was not only the rate controlling step [19,50–52,55–61]. The sorption data indicated that the sorption removal of the fluoride from aqueous phase on to algae was rather complex process, involving both boundary layer diffusion and intraparticle diffusion. The slope of the linear portion was defined as a rate parameter (k_p) and characteristic of the rate of adsorption in this region where intraparticle diffusion was rate limiting is depicted Table 1.



(a)



(b)



(c)

Fig. 4. (a) Intra particle diffusion mode lot of algal–fluoride sorption system [temperature, 30 °C; agitation, 100 rpm; biosorbent mass, 0.1 g; pH 7.0]. (b) Pseudo kinetics plots of algal–fluoride sorption system, pseudo first order [temperature, 30 °C; agitation, 100 rpm; biosorbent mass, 0.1 g; pH 7.0]. (c) Pseudo kinetics plots of algal–fluoride sorption system, pseudo second order [temperature, 30 °C; agitation, 100 rpm; biosorbent mass, 0.1 g; pH 7.0].

3.2.2. Pseudo first and second order models

The pseudo first and second order kinetic models assume that sorption is a pseudo chemical reaction and the sorption rate could be determined, respectively, by the first order and second order reaction rate equations [50].

$$\frac{dq_t}{dt} = k_1(q_e - q_t) \quad (2)$$

$$\frac{dq_t}{dt} = k_2(q_e - q_t)^2 \quad (3)$$

where q_e (mg/l) is the solid phase concentration of the fluoride at equilibrium, q_t (mg/g) the average solid phase concentration of fluoride at contact time (t (min)) and k_1 (min⁻¹) and k_2 (g/mg min) are the pseudo first order and pseudo second order rate constants, respectively. If the sorption followed the pseudo first

Table 1
Summary of sorption data evaluated by different kinetic models

Kinetic model	Initial fluoride concentration (mg/l)	Rate constant	R^2
Pseudo first order kinetic models	5	-0.2448 min^{-1}	0.751
	10	-0.1072 min^{-1}	0.6316
	15	-0.0583 min^{-1}	0.6571
	20	-0.1159 min^{-1}	0.8324
	25	-0.0402 min^{-1}	0.7901
Pseudo second order kinetic model	5	48.01 g/mg min	0.976
	10	12.02 g/mg min	0.980
	15	5.55 g/mg min	0.986
	20	3.51 g/mg min	0.957
	25	2.85 g/mg min	0.985
Intra particle diffusion model	5	0.15 mg/g min ^{0.5}	0.974
	10	0.25 mg/g min ^{0.5}	0.986
	15	0.15 mg/g min ^{0.5}	0.971
	20	0.25 mg/g min ^{0.5}	0.986
	25	0.33 mg/g min ^{0.5}	0.997

order rate equation, a plot of $\ln(q_e - i)$ against contact time ' t ' should be a straight line. Similarly, t/q_t should change linearly with time ' t ' if the sorption process obeyed the pseudo second order rate equation. The derived rate constants together with the correlation coefficient R^2 are depicted in Table 1. (Fig. 4(a and b) display the best-fitting results by the modified pseudo first and second order rate equations, respectively.)

The intraparticle diffusion model generated the best fit with the sorption kinetic data for the investigated fluoride–algal sorption systems, among the three kinetic models evaluated. All the correlation coefficients obtained were larger than 0.97 (Table 1). The modified pseudo second order equation showed next good fit with the sorption data (>0.95), followed by the pseudo first order rate model (>0.63). In the case of pseudo first order rate model, all the correlation coefficients obtained were above 0.63 and less than 0.83 indicating the limited applicability of this model for the investigated algal–adsorption system. The algal–fluoride system was confining to the intraparticle diffusion model along with modified pseudo second order equation. Reported studies showed that the pseudo second order rate equation was a reasonably good fit of the data over the entire fractional approach to equilibrium and therefore was employed extensively in the study of adsorption kinetics [51,52,58,59,62]. The applicability of intraparticle diffusion model suggests that sorptive process of fluoride onto the algal biomass is rather a complex process involving both boundary layer and intraparticle diffusion [19,50]. It could be also presumed from the discussion that the modified pseudo second order equation was potentially a generalized kinetic model for adsorption system under study. The rate constants k_1 [pseudo first order rate constant, min^{-1}] and k_2 [pseudo second order rate constant, $\text{g}/(\text{mg min})$] decreased with increase in the initial concentration of the fluoride in the adsorption systems. On the contrary, the rate constant of the intraparticle diffusion model increased with the increase in the initial concentration of fluoride. The diverse effect of the initial

concentration on k_1 and k_p was also observed with other sorption systems reported [52,63,64].

3.2.3. Adsorption equilibrium

Both Langmuir's and Freundlich's adsorption isotherm equilibrium models were used for the analysis of the algal–fluoride sorption system. The rearranged Langmuir's adsorption isotherm model for evaluating the monolayer sorption phenomena as depicted in Eq. (4) was used to calculate the maximum adsorption capacity of the adsorbent Q_m (mg/g) and a constant (k_a) related to the affinity of the binding sites (l/mg).

$$\frac{C_{\text{eq}}}{q_{\text{eq}}} = \frac{1}{k_a Q_m} + \frac{C_{\text{eq}}}{Q_m} \quad (4)$$

Freundlich's adsorption isotherm model used to study the non-ideal adsorption involving heterogeneous adsorption phenomena was evaluated by the linearised Eq. (5) form

$$\log(q_{\text{eq}}) = \frac{1}{n} \log(C_{\text{eq}}) + \log(k_f) \quad (5)$$

where k_f and $1/n$ are empirical constants. A theoretical plot of the Langmuir's adsorption isotherm model fitted with the experimental data is shown in Fig. 5(a). The experimental data produced a straight line fit with a relatively good correlation coefficient (R^2 0.933) indicating the acceptability of the model for the studied algal–fluoride system. The coefficients obtained from the linearization of the Langmuir's equation exhibited an adsorption capacity (Q_m) of 1.272 mg/g and Langmuir con-

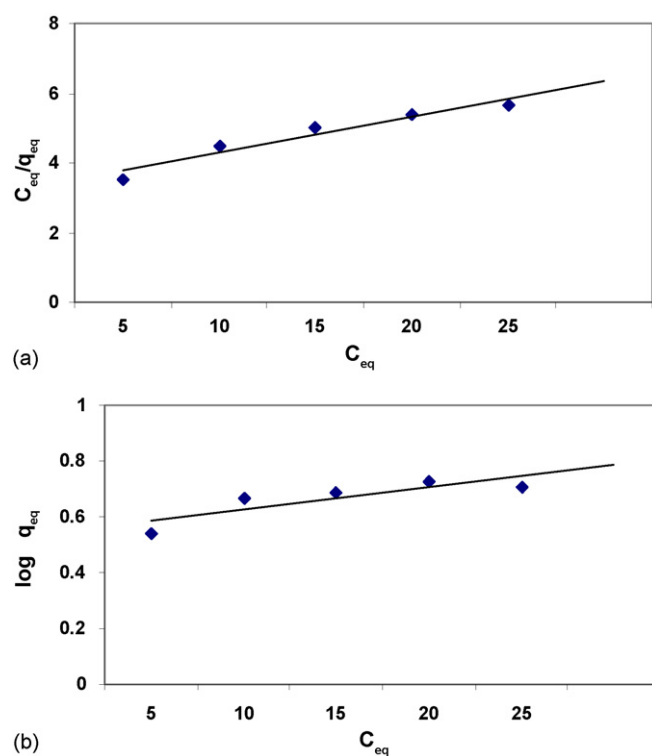


Fig. 5. (a) Langmuir adsorption isotherm plot for algal–fluoride sorption system [temperature, 30 °C; agitation, 100 rpm; biosorbent mass, 0.1 g; pH 7.0]. (b) Freundlich adsorption isotherm plot for algal–fluoride sorption system [temperature, 30 °C; agitation, 100 rpm; biosorbent mass, 0.1 g; pH 7.0].

stant (K_a) of 0.585 mg^{-1} as can be seen from Fig. 5(b). The transformation of experimental data to Freundlich's adsorption isothermal model did not lead to linearization (R^2 0.709) indicating the non acceptability of isothermal model.

Hall et al. [65] and Venkata Mohan et al. [19] showed that essential characteristics of a Langmuir adsorption isotherm equation could be expressed in terms of a dimensionless constant called as separation factor or equilibrium factor or equilibrium parameter, 'Rs' which was defined by the following equation,

$$R_s = \frac{1}{1 + aC_0} \quad (6)$$

where, R_s is the dimensionless constant separation factor; a the Langmuir's constant as defined earlier (μg); and C_0 is the initial solute concentration ($\mu\text{g/l}$). The separation factor as described by Hall et al. [65] was calculated using the Langmuir's model constants. By the separation factor value the value of the isotherm can be assessed by following classification [66] as shown below:

- $R_s > 1$: unfavorable isotherm;
- $R_s = 0$: linear isotherm;
- $0 < R_s < 1$: favorable isotherm;
- $R_s < 0$: irreversible isotherm.

' R_s ' was calculated for the linearised Langmuir's adsorption isotherm and was found to be 0.253, for algal fluoride sorption system, which was considered to be a favorable condition.

3.3. Influence of pH

Biosorption process is dependent on the aqueous phase pH and the functional groups on the algal cell walls and their ionic states (at particular pH) determine the extent of biosorption [35,42,64,67,68]. The algae cell wall contains a high amount of polysaccharides and some of them are associated with proteins and other components [25,27,29,69]. These biomacromolecules on the algal cell surfaces have several functional groups (such as, amino, carboxyl, thiol, sulfhydryl and phosphate groups) and biosorption phenomena depends on the protonation or un protonation of these functional groups on the surface of the cell wall [25]. The ionic form of fluoride in solution and the electrical charge of the algal cell wall components (i.e., functional groups carrying polysaccharides and proteins) depend on the solution pH. Batch sorption experiments were performed at various aqueous phase pH (2.0, 5.0, 6.0, 7.0, 8.5 and 10.5) by keeping all other experimental conditions constant [temperature, 30°C , agitation, 100 rpm; biomass, 0.1 g; concentration, $5 \text{ mg F}^-/\text{l}$; agitation, 100 rpm]. The effect of pH on the adsorptive removal of fluoride ion with the function of contact time is depicted in Fig. 6. The extent of fluoride sorption on the algal sorption system showed a marked decrease as the pH of the aqueous solution increased from 2.0 to 10.5. The highest biosorption values were observed at pH 2.0 (62%) where the overall surface charges on the algal cells should be positive, which facilitated the binding of negatively charged fluoride ion. This specific phenomenon of sorption characteristics could be

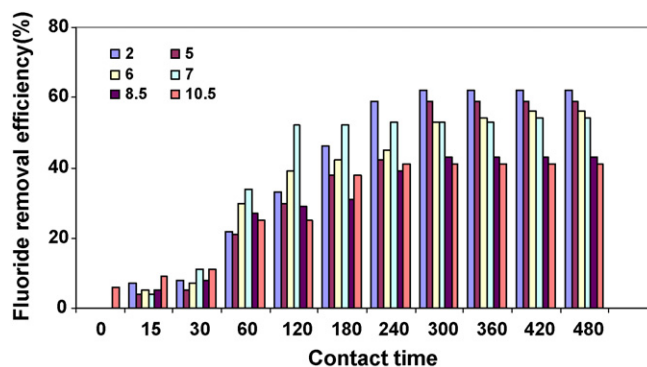


Fig. 6. Influence of aqueous phase pH on sportive removal of fluoride [temperature, 30°C ; agitation, 100 rpm; biosorbent mass, 0.1 g; concentration, $5 \text{ mg F}^-/\text{l}$].

attributed to the anionic sorption, which indicated that the adsorbent surface is of H^+ (cationic)-type [50]. At lower pH values, the surface of the adsorbent turned out to be positively charged and this facilitated sorption of fluoride ions, probably by the anionic exchange sorption. At acidic pH due to the protonated effect of surface functional groups such as amino, carboxyl, thiol, etc., imparts positive charge on the surface [25]. Relative sorption inhibition observed at basic pH range might be attributed to the increase of hydroxyl ion leading to formation of aqua-complexes thereby retarding the sorption [35]. However, the fluoride sorption efficiency at aqueous phase pH 7.0 was found to be 54%, which is considered to be on higher side and cannot be avoided for all practical reasons with respect to the upscaling of the technology.

3.4. Influence of temperature

The influence of aqueous phase temperature on the biosorption experiments was investigated at five different temperatures (10, 20, 30, 40 and 50°C) by keeping all other experimental conditions constant [pH 7.0, agitation, 100 rpm; biomass, 0.1 g; concentration, $5 \text{ mg F}^-/\text{l}$; agitation, 100 rpm]. The effect of aqueous phase temperature on the fluoride ion removal by algal biosorbent was shown in Fig. 7. An increase in sorption

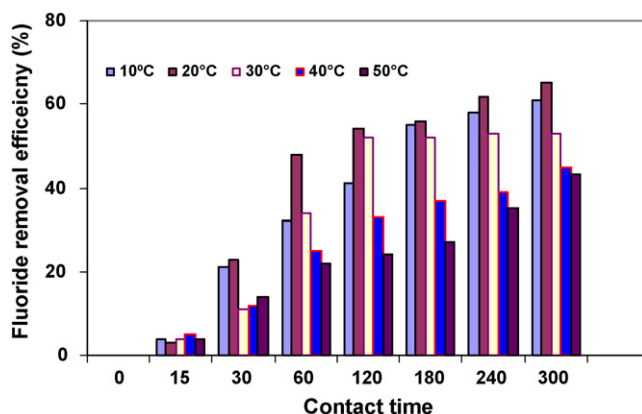


Fig. 7. Influence of temperature on the algal sorption capacity [pH 7; agitation, 100 rpm; biosorbent mass, 0.1 g; concentration, $5 \text{ mg F}^-/\text{l}$].

capacity was observed with increasing temperature from 10 to 50 °C. An apparent sorption (F^-) rate acceleration on raising the temperature was reported by Liang et al. [70], Meena et al. [71] reported that the increase in sorption with temperature may be attributed to either increase in the number of active surface sites available for sorption on the adsorbent or due to the decrease in the boundary layer thickness surrounding the sorbent, so that the mass transfer resistance of adsorbate in the boundary layer decreased.

3.5. Adsorption–desorption/reuse studies

Adsorption–desorption experiments are useful in elucidation of the mechanism of sorption reaction and also to assess the regeneration capacity of the adsorbent for reuse in a more economic manner. Three consecutive cycles of adsorption–desorption experiments were carried out separately with three different desorption solvents (0.1N HCl, 0.1N NaOH and distilled water) (Fig. 8). The amount of desorption provides an insight into the nature of adsorbent–adsorbate bonding and also on the ion exchange property of the adsorbent. Comparatively effective desorption of fluoride ions from biomass was found in acidic solution. However, the desorption in the case of distilled water and 0.1N NaOH was slightly on lower side in all the cycles studied. The resultant desorption phenomenon observed in both distilled water and inorganic solvents might be attributed to both physical (desorption in distilled water in which fluoride ions are bound to the surface by weak bonding) and ion exchange type (desorption in inorganic solvents) interaction rather than chemical sorption [72]. The combined effect of ion exchange and physical sorption phenomena might be possible during the fluoride–algal sorption, which can be corroborated with the observation from pH studies reported in earlier section. A consistent reduction in adsorption capacity was noticed for each new cycle after desorption (Fig. 8). With three cycles, the adsorption capacity reduced by ~20% from 62% (distilled water), 64% (0.1N HCl) and 60% (0.1N NaOH) to 40% (distilled water), 44% (0.1N HCl) and 40% (0.1N NaOH). Furthermore, relatively effective reusability was noticed when the loaded biomass was desorbed with 0.1N HCl solvent (Fig. 8).

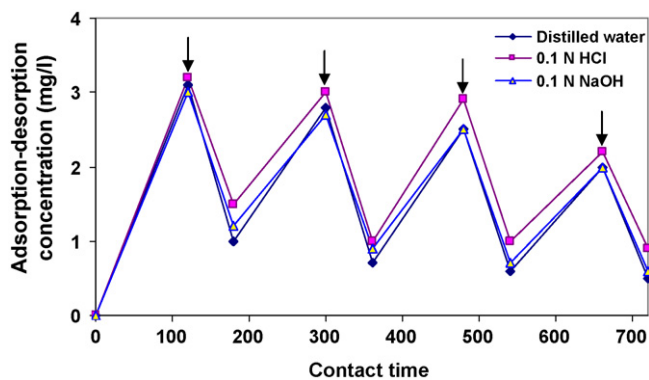


Fig. 8. Pattern of adsorption–desorption of fluoride [temperature, 30 °C; agitation, 100 rpm; biosorbent mass, 0.1 g; concentration, 5 mg F^- /l; adsorption (contact) time, 120 min; desorption time, 60 min] (↓ represents desorption).

Table 2
Surface function group observed on algal biosorbent by FT-IR spectroscopy

Before acid treatment (cm^{-1})	After the acid treatment (cm^{-1})	After adsorption (cm^{-1})	Bonds indicative of
3411	3411	3412	OH stretch/carboxylic
2926	2925	2924	Carboxylic/phenolic
1644	1656	1642	$>C=N-$, $>C=C$ C, $C=O$ stretch
1541	1549	1540	Quinone OH bonds
1924	1430	1400	
1240	1237	1245	C–O–
–	1161	1163	$=C-C=$
1059	1059	1060	$\equiv C-N<$
–	–	1000	$-C-F$ stretch
8733	–	873	Plane deformation
–	664	666	
613	614	614	
460	464	464	

On the whole the overall cumulative fluoride sorption observed for the three cycles was 10.4 mg F^- /l (distilled water), 11.3 mg F^- /l (0.1N HCl) and 10.2 mg F^- /l (0.1N NaOH). However, due to relatively less variation and on economical point of view distilled water could be used as desorption solvent for the studied algal–fluoride adsorption system.

3.6. Sorption elucidation

3.6.1. FT-IR analysis

FT-IR spectra were obtained for the algal biosorbent before and after acid treatment and after fluoride adsorption were performed and the resulting surface functional groups were depicted in Table 2. Interpretations of the spectra were based on the infor-

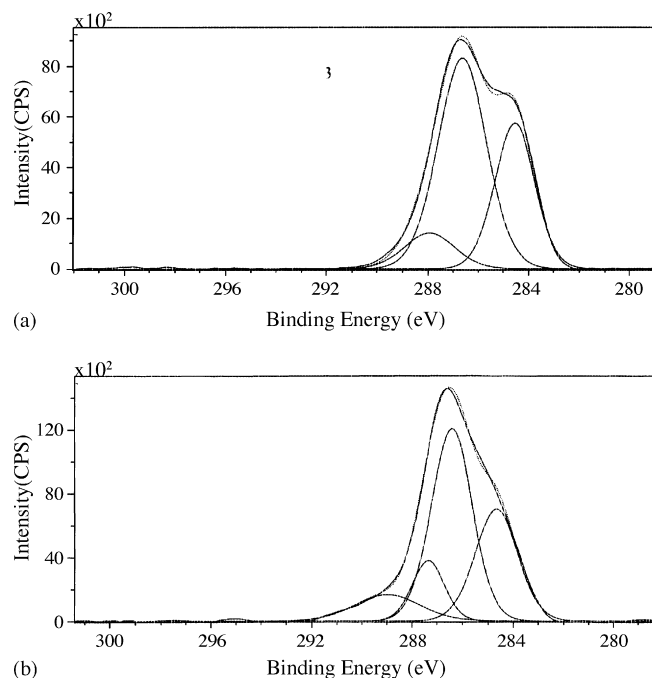


Fig. 9. XPS spectra (a) before sorption and (b) after sorption.

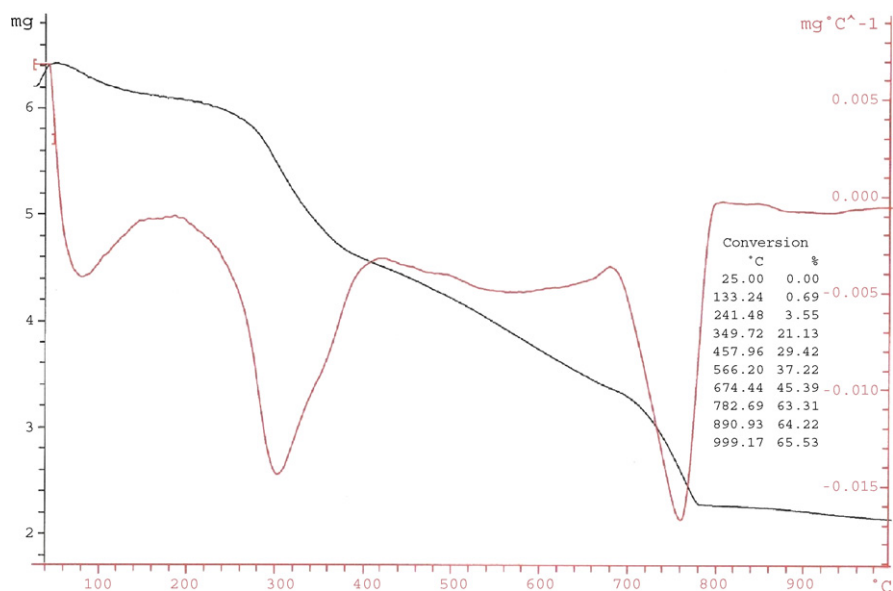


Fig. 10. Thermal analysis profile of biosorbent after fluoride sorption.

mation acquired from literature [73–80]. Significant changes in the FT-IR spectra after the fluoride sorption were found at the wave numbers of 3412, 2924, 1642, 1540, 1400, 1245, 1163, 1060 and 1000 cm^{-1} . Display of strong broad O–H stretch carboxylic bands in the region 3412 cm^{-1} and carboxylic/phenolic stretching bands in the region of 2924 cm^{-1} was observed. The bands appeared in the region 1642 cm^{-1} might be attributed to $>\text{C}=\text{N}$, $>\text{C}=\text{C}$ C and $\text{C}=\text{O}$ stretch. The bands appeared in the region of 1540 and 1400 cm^{-1} might be attributed to the presence of quinine and OH bonds. The bands appearing in the region 1245, 1163, 1060 and 1000 cm^{-1} indicated the presence of $-\text{C}-\text{O}-$, $=\text{C}-\text{C}=\text{}$, $\equiv\text{C}-\text{N}<$ and $-\text{C}-\text{F}$ stretch groups, respectively. FT-IR results indicated that mainly hydrogen atoms in the carboxylic groups were involved in fluoride ion sorption. This observation correlated well with the desorption and pH studies data.

3.6.2. XPS analysis

Surface properties play an important role in numerous important technologies. X-ray photoelectron spectroscopy (XPS) is a widely used method for surface analysis of materials, due to its surface sensitivity and chemical specificity. From the XPS spectra, the elements present and their chemical state (valence) can be determined. Since only electrons emitted from atoms near the surface escape without losing energy, this technique is surface sensitive. Subtle changes in peak positions and shape can yield important information on changes in surface chemistry, giving XPS the ability to determine the elemental composition on the surface of materials. Analysis of the XPS data gave an idea about the local oxidation states and chemical bonding environment of the composing material. Fig. 9 shows the high resolution scans for C 1s of biosorbent *Spirogyra IO2* before and after fluoride sorption. XPS survey scan of *Spirogyra* sample 1 showed peaks characteristic of O 1s, C 1s, N 1s, S 2p and P 2p at 532, 284, 400, 164 and 135 eV, respectively. In *Spirogyra* loaded with fluoride in addition to the above peaks a peak at 685 eV was

observed which could be attributed to F 1s that is adsorption. In virgin biosorbent the observed C 1s peak could be convoluted into three peaks at 284.6 eV (32.5%), 286.6 eV (57.3%) and 287.9 eV (10.2%), which could be attributed to the presence of $\text{C}-\text{C}/\text{C}-\text{H}$, $-\text{O}-\text{C}-\text{O}-$, and carboxylic group ($-\text{O}-\text{C}=\text{O}-$), respectively. After sorption with fluoride the C 1s XPS high resolution narrow scan showed peak at 284.6 eV (29.3%), 286.5 eV (48.1%), 287.4 eV (11.9%) and 288.9 eV (10.7%). The peak observed at 288.9 eV was attributed to the $-\text{CH}_2-\text{CF}_2-$ bond formation. The areas under the curve showed a marginal increase in the area for the binding energy peak at 287.4 eV could be attributed to a component from the formation of $-\text{C}-\text{F}-$ bonds.

3.6.3. TGA analysis

Thermo gravimetric (TGA) analysis of the fluoride loaded biosorbent (Fig. 10) showed that the biosorbent underwent three steps decomposition process when heated from 25 to 100 $^{\circ}\text{C}$. Initial step ($\sim 1\%$ weight loss), which was small in the range in 25–150 $^{\circ}\text{C}$ could be attributed to the loss of adsorbed water ($\sim 65\%$) molecules. Maximum weight loss due to degradation was observed in the next two steps, i.e., between 200 and 400 $^{\circ}\text{C}$ and 700 and 800 $^{\circ}\text{C}$ indicating that the organic fraction of the studied biosorbent got decomposed in this range.

4. Conclusions

Adsorption studies performed on the algal *Spirogyra IO2* sp. as biosorbents revealed the ability of algal species to remove fluoride from the aqueous phase. Batch sorption studies performed on the algal–fluoride sorption system indicated varied fluoride sorption capacity. Fluoride–algal interaction concurred showed good fit with pseudo first order rate equation. Isothermal data fitted well with the Langmuir’s adsorption isotherm model. Effect of pH was documented while desorption was more evident in inorganic solution and distilled water. FT-IR spectral studies and X-ray photoelectron spectroscopy (XPS) analysis were

conducted on virgin and fluoride loaded biosorbent to understand fluoride algal sorption mechanism. Thermo gravimetric (TGA) analysis was also performed on fluoride loaded biosorbent to study the temperature imbedded degradation nature of the biosorbent and to assess its disposal nature.

References

- [1] S. Venkata Mohan, P. Nikhila, S.J. Reddy, Determination of fluoride content in drinking water and development of a model in relation to some water quality parameters, *Fresen. Environ. Bull.* 4 (1995) 297–302.
- [2] H.E. Short, G.R. Mc Robert, T.W. Bernard, A.S. Mannadiyar, Endemic fluorosis in the madras presidency, *Ind. J. Med. Res.* 25 (1937) 553–561.
- [3] Sangam, Combating fluorosis with household filters, Newsletters of UN inter agency-working group on water and environmental sanitation in India (UNICEF), (2003) 1–2.
- [4] K. Sarala, P.R. Rao, Endemic fluorosis in the Village Ralla, Anantapuram in Andhra Pradesh—an epidemiological study, *Fluoride* 26 (1993) 177–180.
- [5] A.K. Susheela, A. Kumar, M. Betnagar, M. Bahadur, Prevalence of endemic fluorosis with gastro-intestinal manifestations in people living in some north-Indian villages, *Fluoride* 26 (1993) 97–104.
- [6] WHO, Health Criteria and Other Supporting Information, Guidelines for Drinking Water Quality, CBS Publishers and Distributors, 1985, p. 2.
- [7] S.V. Ramanaiah, S. Venkata Mohan, B. Rajkumar, P.N. Sarma, Monitoring of fluoride concentration in ground water of Prakasham District in India; correlation with physico chemical parameters, *J. Environ. Sci. Eng.* (2006), accepted for publication.
- [8] B.K. Handa, Geochemistry and genesis of fluoride containing groundwater in India, *Ground Water* 13 (1975) 278–281.
- [9] A.M. Raichur, M. Jyoti Basu, Adsorption of fluoride onto mixed rare earth oxides, *Sep. Purif. Technol.* 24 (2001) 121–127.
- [10] E.J. Reardon, Y. Wang, Limestone reactor for fluoride removal from waste waters, *Environ. Sci. Technol.* 34 (2000) 3247–3253.
- [11] S. Saha, Treatment of aqueous effluent for fluoride removal, *Water Res.* 27 (1993) 1347–1350.
- [12] G. Singh, B. Kumar, P.K. Sen, J. Maunder, Removal of fluoride from spent pot liner leachate using ion exchange, *Water Environ. Res.* 71 (1999) 36–42.
- [13] A. Dieye, C. Larchet, B. Auclair, C. Mar-Diop, Elimination des fluorures par la dialyse ionique croisée, *Eur. Polym. J.* 34 (1998) 67–75.
- [14] Z. Amer, B. Bariou, N. Mameri, M. Taky, S. Nicolas, A. Elimidaoui, Fluoride removal from brackish water by electro dialysis, *Desalination* 133 (2001) 215–223.
- [15] N. Mameri, H. Lounici, D. Belhocine, H. Grib, D.L. Prion, Y. Yahiat, Defluoridation of Sahara Water by small electro coagulation using bipolar aluminium electrodes, *Sep. Purif. Technol.* 24 (2001) 113–119.
- [16] M. Hichour, F. Persin, J. Sandeaux, C. Gavach, Water defluoridation by Donnan Dialysis and electro dialysis, *Sep. Purif. Technol.* 18 (2000) 1–11.
- [17] M. Hichour, F. Persin, J. Sandeaux, C. Gavach, Water defluoridation by Donnan Dialysis and electro dialysis, *Rev. Sci. Eau.* 12 (1999) 671–686.
- [18] S.K. Adikari, U.K. Tipnis, W.P. Harkare, K.P. Govindan, Defluoridation during desalination of brackish water by electro dialysis, *Desalination* 71 (1989) 301–312.
- [19] S. Venkata Mohan, N. Chandrasekhar Rao, J. Karthikeyan, Adsorption removal of direct azo dye aqueous phase onto coal based sorbents—a kinetic and mechanistic study, *J. Hazard. Mater.* 90 (2) (2002) 189–204.
- [20] K.S. Jayantha, G.R. Ranjana, H.R. Sheela, R. Modang, Y.S. Shivanani, Defluoridation studies using laterite material, *J. Environ. Sci. Eng.* 46 (4) (2004) 282–288.
- [21] N. Prabavathi, T. Ramachandramoorthy, R. Edison Raja, B. Kavitha, C. Sivaji, R. Srinivasan, Drinking water of Salem district—estimation of fluoride and its defluoridation using lignite rice husk and rice-husk powder, *IJEP* 23 (3) (2003) 304–308.
- [22] S. Srimurali, A. Pragathi, J. Karthikeyan, A study on removal of fluorides from drinking water by adsorption onto low-cost materials, *J. Environ. Pollut.* 99 (1998) 285–289.
- [23] K. Muthukumar, K. Balasubramanian, T.V. Ramakrishna, Removal of fluoride by chemically activated carbon, *IJEP* 15 (7) (1995) 514–517.
- [24] D.J. Killedar, D.S. Bhargava, Effects of stirring rate and temperature on fluoride removal by fishbone charcoal, *Ind. J. Environ. Health* 35 (2) (1993) 81–87.
- [25] T. Ilhami, B. Gulay, Y. Emine, B. Gokben, Equilibrium and kinetic studies on biosorption of Hg(II), Cd(II) and Pb(II) ions onto micro algae *Chlamydomonas reinhardtii*, *J. Environ. Manag.* 77 (2005) 85–92.
- [26] R. Gupta, P. Ahuja, S. Khan, R.K. Saxena, H. Mohapatra, Microbial biosorbents: meeting challenges of heavy metal pollution in aqueous solutions, *Curr. Sci.* 78 (2000) 967–973.
- [27] C.J. Williams, R.G.J. Edyvean, Ion exchange in nickel biosorption by seaweed materials, *Biotechnol. Prog.* 13 (1997) 424–428.
- [28] A.P. McHale, S. McHale, Microbial biosorption of metals, potential in the treatment of metal pollution, *Biotechnol. Adv.* 12 (1994) 647–652.
- [29] L.E. Macaskie, A.C.R. Dean, *Biological Waste Treatment*, Alan R. Liss, New York, 1989, 159–201.
- [30] G.M. Gadd, in: H.J. Rehm, G. Reed (Eds.), *Biotechnology—A Comprehensive Treatise, Special Microbial Processes*, vol. 6b, VCH, Verlagsgesellschaft, Weinheim, Germany, 1988, pp. 401–433.
- [31] L.E. Macaskie, A.C.R. Dean, Uranium accumulation by immobilized cells of a *Citrobacter* sp., *Biotechnol. Lett.* 7 (1985) 457–462.
- [32] M. Tsezos, B. Volesky, Mechanism of uranium biosorption by *Rhizopus arrhizus*, *Biotechnol. Bioeng.* 24 (385) (1982) 401.
- [33] B. Volesky, Z.R. Holan, Biosorption of heavy metals, *Biotechnol. Prog.* 11 (1995) 235–250.
- [34] L. Arjun Khandare, P. Uday Kumar, G. Shankar, K. Venkaiah, N. Laxmaiah, Additional beneficial effects of Tamarind ingestion over defluoridated water supply to adolescent boys in a fluorotic area, *Nutrition* 20 (2004) 433–436.
- [35] S. Venkata Mohan, Y. Vijaya Bhaskar, J. Karthikeyan, Biological decoloration of simulated azo dye in aqueous phase by algae *Spirogyra* species, *Int. J. Environ. Pollut.* 21 (3) (2003) 211–222.
- [36] B. Jamode, S. Chandak, M. Rao, Evaluation of performance and kinetic parameters for defluoridating using *Azadirachta Indica* (neem) leaves as low cost adsorbents, *Pollut. Res.* 23 (2) (2004) 239–250.
- [37] T. Ramachandra Murthy, D.A. Jeyakar, R. Chellaraj, T. Edison Raja, R. Venkatachalam, Sangeetha, C. Sivaraj, Fluoride estimation in potable water in Tiruchirapalli Rock—Port Area—Dental fluorosis survey and Defluoridation with Emblicaphyllanth, *IJEP* 239 (3) (2003) 317–320.
- [38] L. Udaya Simha, B. Panigrahy, S.V. Ramakrishna, Preliminary studies on fluoride adsorption by water hyacinth, *IJEP* 22 (5) (2002) 506–511.
- [39] P. Mariappan, V. Yegnamaran, T. Vasudevan, Defluoridation of using low cost activated carbons, *IJEP* 22 (2) (2000) 154–160.
- [40] S. Venkata Mohan, N. Chandrasekhar Rao, K. Krishna Prasad, J. Karthikeyan, Treatment of simulated reactive yellow 22 (azo) dye effluents using *Spirogyra* species, *Waste Manag.* 22 (2002) 575–582.
- [41] S. Venkata Mohan, J. Karthikeyan, Removal of diazo dye from aqueous phase by algae *Spirogyra* species, *Toxicol. Environ. Chem.* 74 (2000) 147–154.
- [42] R.S. Prakasam, P.L. ChandraReddy, A. Manisha, S.V. Ramakrishna, Defluoridation of drinking water using eichhornia SP, *IJEP* 19 (2) (1998) 119–124.
- [43] M. Bhatnagar, A. Bhatnagar, S. Jha, Interactive biosorption by micro algal biomass as a tool for fluoride removal, *Biotechnol. Lett.* 24 (2002) 1079–1081.
- [44] M. Bhatnagar, A. Bhatnagar, Algal and cyanobacterial responses to fluoride, *Fluoride* 33 (2) (2000) 55–65.
- [45] K.T. Semple, R.B. Cain, S. Schmidt, Biodegradation of aromatic compounds by micro algae, *FEMS Microb. Lett.* 176 (2) (1999) 291–301.
- [46] A. Kapoor, T. Viraraghavan, Biosorption of heavy metals *Aspergillus Niger*, effect of pretreatment, *Biores. Technol.* 63 (1998) 109–113.
- [47] K.M. Paknikar, U.S. Palnitkar, P.R. Puranik, Biohydrometallurgical technologies, in: A.E. Torma, M.L. Apel, C.L. Brierley (Eds.), *The Minerals, Metals and Materials Society*, vol. II, TMS Publications, Wyoming, USA, 1993, pp. 229–236.
- [48] B. Greene, D.W. Darnall, in: H.L. Ehrlich, C.L. Brierley (Eds.), *Microbial Mineral Recovery*, McGraw Hill, 1990, pp. 277–301.

- [49] APHA, Standard Methods for Examination of Water and Wastewater, 20th ed., American Public Health Association, Washington, DC, 1998.
- [50] S. Venkata Mohan, J. Karthikeyan, Removal of lignin and tannin aqueous solution by adsorption onto activated charcoal, *Environ. Pollut.* (1–2) (1997) 183–197.
- [51] X. Yang, B. Al-Duri, Kinetic modeling of liquid-phase adsorption of reactive dyes on activated carbon, *J. Colloid Interface Sci.* 287 (2005) 25–34.
- [52] M. Yalcin, A. Gurses, C. Dogar, M. Sozbilir, The adsorption kinetics of cetyl tri methyl ammonium bromide (CTAB) onto powdered active carbon, *Adsorption* 10 (2004) 339–348.
- [53] C.Y. Chang, W.T.T. Sai, C.H. Ing, C.H. Chang, Adsorption of polyethylene glycol (PEG) from aqueous solution onto hydrophobic zeolite, *J. Colloid Interface Sci.* 260 (2003) 273–279.
- [54] C.L. Brierley, H.L. InEhrlich, C.L. Brierly (Eds.), *Microbial Mineral Recovery*, McGraw-Hill, New York, 1990, pp. 303–324.
- [55] A.S. Ozcan, B. Erdem, B. Ozcan, Adsorption of Acid Blue 193 from aqueous solutions onto Na-bentonite and DTMA-bentonite, *J. Colloid Interface Sci.* 280 (2004) 44–54.
- [56] F.C. Wu, R.-I. Tseng, R.-S. Jung, Kinetic modeling of liquid-phase adsorption of reactive dyes and metal ions on chitosan, *Water Res.* 35 (2001) 613–618.
- [57] M.M.F. Figucira, B. Volesky, V.S.T. Cininelli, Biosorption of metals in brown seaweed biomass, *Water Res.* 34 (2000) 196–204.
- [58] L.E. Malaskie, A.C.R. Dean, in: B. Molesky (Ed.), *Metals-sequestering Biochemicals, Biosorption of Heavy Metals*, CRC press, Boca Raton, FL, 1990, pp. 199–248.
- [59] S.A. Brierley, B.In. Volesky (Eds.), *Reduction and Application of a Bacillus-Based Product for Use in Metal Biosorption, Biosorption of Heavy Metals*, CRC Press, Boca Raton, FL, 1990, pp. 305–312.
- [60] W.J. Weber Jr., *Physico-chemical Processes for Water Quality Control*, John Wiley, New York, 1972.
- [61] E. Perial, R.H. McDowell, *Chemistry and Enzymology of Marine Algal Polysaccharides*, Academic Press, London, 1967, pp. 99–126.
- [62] S. Hunt, B.In. Eeels, S. Hunt (Eds.), *Diversity of Biopolymers Structure and Its Potential for Ion-bonding Applications, Immobilization of Ions by Biosorption*, Ellies Horword, Chichester, 1996, pp. 15–45.
- [63] S. Venkata Mohan, S.V. Ramanaiah, B. Rajkumar, P.N. Sarma, Biosorption of fluoride from aqueous phase onto algal *Spirogyra* IO1 and evaluation of adsorption kinetics, *Bioresour. Technol.* (2006), Available online at www.sciencedirect.com.
- [64] J. Crack, *The Mathematics of Diffusion*, Clarendon press, London, 1965.
- [65] K.R. Hall, L.C. Eagleton, A. Acirios, T. Vermeulen, Pore and solid diffusion kinetics in fixed bed adsorption under constant pattern conditions, *I & EC Fundamentals* 5 (1966) 212–223.
- [66] T.W. Weber, P.K. Chakravorti, Pore and solid diffusion models for fixed adsorbors, *AIChE J.* 20 (1974) 226–237.
- [67] O. Genc, Y. Yalcinkaya, Buyuktuncel, A. Denizli, M.Y. Arica, S. Bektas, Uranium recovery by immobilized and dried powdered biomass, characterization and comparison, *Int. J. Miner. Process* 68 (2003) 93–107.
- [68] E.W. Wilde, J.R. Benemann, Bioremoval of heavymetals by the use of microalgae, *Biotechnol. Adv.* 11 (1993) 781–812.
- [69] R.H. Crist, K. Oberholser, N. Shank, M. Nguyen, Nature of binding between metallic ions and algal cell walls, *Environ. Sci. Technol.* 15 (1981) 1212–1217.
- [70] L.V. Liang, J. He, M. Wei, D.G. Evans, X. Duan, Factors influencing the removal of fluoride from aqueous solution by calcined Mg-Al-Co₃ layered double hydroxides, *J. Hazard. Mater. B* 113 (2006) 119–128.
- [71] A.K. Meena, G.K. Mishra, P.K. Rai, C. Rajagopal, P.N. Nagar, Removal of heavy metal ions from aqueous solutions using carbon aero gel as an adsorbent, *J. Hazard. Mater. B* 122 (2005) 161–170.
- [72] S. Venkata Mohan, Removal of textile dye colour from aqueous solution by adsorption onto coal/coal based sorbents, PhD Thesis, 1997, Sri Venkateswara University, Tirupati, India.
- [73] S. Venkata Mohan, S.K. Mohan, J. Karthikeyan, IR, XRD and SEM studies to elucidate the mechanism of azo dye sorption interaction with coal based adsorbents and activated carbon from aqueous phase, *J. Sci. Ind. Res.* 60 (2001) 410–415.
- [74] H.P. Boehm, Some aspects of the surface chemistry of carbon blacks and other carbons, *Carbon* 35 (1994) 759–769.
- [75] J. Zawadzki, Infrared studies on aromatic compounds adsorbed on the surface of carbon films, *J. Colloidal Interface Sci.* 26 (1998) 603–614.
- [76] C. Ishizaki, I. Marti, Surface oxide structures on a commercial activated carbon system, *J. Colloidal Interface Sci.* 19 (1981) 409.
- [77] J.S. Mattson, H.B. Mark, *Activated Carbon-Surface Chemistry and Adsorption from Solution*, Marcel Dekker Inc., New York, USA, 1971.
- [78] J.S. Mattson, H.J. Mark, Infrared internal reflectance spectroscopic determination of surface functional groups on carbon, *J. Colloidal Interface Sci.* 31 (1969) 131–144.
- [79] J.S. Mattson, H.B. Mark Jr., W.J. Weber, Identification of surface functional groups on active carbon by infrared reflection spectrophotometer, *Anal. Chem.* 41 (1969) 355–358.
- [80] V.I. Snoeyink, W.J. Weber, The surface chemistry of active carbon—a discussion of structure and surface functional groups, *Environ. Sci. Technol.* 1 (1967) 249–254.